

Radio-photoluminescence Properties of Eu-doped CaBPO₅

Hirozumi Ito,¹ Go Okada,^{1*} Yasuhiro Koguchi,^{2,1}
Wataru Kada,³ Kenichi Watanabe,⁴ and Hidehito Nanto^{1,2}

¹Co-creative Research Center of Industrial Science and Technology, Kanazawa Institute of Technology,
3-1 Yatsukaho, Hakusan, Ishikawa 924-0838, Japan

²Oarai Research Center, Chiyoda Technol Corporation,

3681 Narita-cho, Oarai-machi, Higashi-ibaraki-gun, Ibaraki 311-1313, Japan

³Department of Quantum Science and Energy Engineering, Tohoku University,

6-6-01-2 Aramaki-Aza-Aoba, Aoba, Sendai, Miyagi 980-8579, Japan

⁴Department of Applied Quantum Physics and Nuclear Engineering, Kyushu University,
744 Motooka, Nishi-ku, Fukuoka 819-0395, Japan

(Received October 31, 2023; accepted January 16, 2023)

Keywords: radio-photoluminescence, RPL, Europium, CaBPO₅

Eu-doped CaBPO₅ was synthesized by the solid-state reaction route, and then its radio-photoluminescence properties were studied. On the basis of steady-state and time-resolved photoluminescence (PL) studies, it was confirmed that Eu²⁺ is formed by X-ray irradiation due to the valence change of the Eu ion (Eu³⁺ → Eu²⁺). In addition, for dosimetric applications, it was demonstrated that the PL intensity of Eu²⁺ is proportional to the accumulated radiation dose, is stable after irradiation, and can be reversed by heat treatment at 500 °C for 100 s.

1. Introduction

Radio-photoluminescence (RPL) has attracted considerable attention in luminescence dosimetry applications.^(1–3) RPL is a phenomenon whereby a luminescence center is formed via interactions with ionizing radiation. The luminescence center formed can be detected by a conventional photoluminescence (PL) technique, and the luminescence intensity is used as a probe of radiation dose since the number of luminescence centers generated (i.e., luminescence intensity) is proportional to the accumulated radiation dose. Despite the usefulness of RPL, conventional materials considered for radiation dosimetry are limited to Ag-doped phosphate glass,^(4–6) LiF,^(7,8) and Al₂O₃:C,Mg.^(9,10) In contrast, recent studies of exploring new RPL materials revealed additional choices such as Sm-doped,^(11–18) Eu-doped,^(19–22) and Yb-doped⁽²³⁾ compounds, as well as undoped compounds.^(24–27)

In this study, as part of the quest for new RPL materials, we have synthesized Eu-doped CaBPO₅ by the solid-state reaction route, and then we found that it exhibits RPL. Furthermore, the origin of RPL as well as the properties for dosimetric applications were discussed in detail.

*Corresponding author: e-mail: go.okada@neptune.kanazawa-it.ac.jp
<https://doi.org/10.18494/SAM4765>

2. Materials and Methods

Eu-doped CaBPO_5 was synthesized by the solid-state reaction route. CaCO_3 (99.99%), $\text{NH}_4\text{H}_2\text{PO}_4$ (99.999%), H_3BO_3 (99.99%), and Eu_2O_3 (99.9%) were first weighed to the stoichiometric ratio and then homogeneously mixed by mortar and pestle for 20 min together with 10 mol.% Na_2CO_3 (99.9%) as a sintering aid. Next, the mixture was loaded to an alumina crucible and then sintered in air at 200 °C for 2 h, followed by 950 °C for 4 h using an electric furnace (FT-101FMW, Full-Tech). The PL excitation spectrum of the obtained sample was characterized using a spectrofluorometer (F-4500, Hitachi). The time-resolved PL spectrum and PL decay curve were obtained using a 349 nm pulse laser (Explore One 349-120, Spectra Physics) as an excitation source, a multichannel spectrometer (PMA-12, Hamamatsu) to obtain a spectrum, and a delay generator (DG535, Stanford Research Systems). The details of the instrumental setup can be found elsewhere.⁽²⁸⁾ Furthermore, to characterize RPL properties, X-ray irradiation, PL spectrum measurement, and thermal treatment were performed using the TSL/OSL/RPL Automated and Integrated Measurement System (TORAIMS).⁽²⁹⁾

3. Results and Discussion

The obtained material was found to be a single phase of CaBPO_5 , and no impurity phase associated with Na was found by X-ray diffraction analysis. The PL properties of the Eu-doped CaBPO_5 are summarized in Fig. 1. Figure 1(a) shows the PL emission and excitation spectra of as-prepared (0 Gy) and X-ray-irradiated (5 Gy) samples. The PL spectrum of the as-prepared sample consists of a strong emission band peaking at 400 nm as well as multiple sharp emission lines across 600–700 nm. The former emission is accompanied by a broad excitation feature across 200–350 nm, while the excitation spectrum of the latter emission feature consists of a broad band across 200–300 nm and sharp peaks at 318, 365, and 394 nm. The comparison of the emission intensities between the as-prepared and X-ray-irradiated samples shows that the 400 nm band is stronger, whereas the 600–700 nm peaks are slightly smaller after X-ray irradiation (5 Gy). To study the above luminescence origins, time-resolved PL spectra and PL decay curves are characterized. Figure 1(b) shows the time-resolved PL spectra of the nanosecond and millisecond ranges. From the spectra of the nanosecond range, it is shown that the 400 nm emission band decays very rapidly, whereas the 600–700 nm emission band remains unchanged. In the millisecond range, however, a decay of the 600–700 nm emission band is clearly demonstrated. In Fig. 1(c), the intensities of these two sets of emissions are plotted as a function of time after pulse excitation. The square-root curve fitting with a single exponential decay function reveals that the 400 nm emission band has a lifetime of 118 ns, whereas the latter emission lines across 600–700 nm have a lifetime of 2.6 ms. It is commonly known that Eu can take its valence state to be either divalent or trivalent. On the basis of the above observations of the spectrum features and lifetime, it is reasonable to assign the luminescence origin of the 600–700 nm emission to the 4f-4f transitions of Eu^{3+} . In contrast, the origin of the 400 nm emission band is considered to be the 5d→4f transitions of Eu^{2+} based on the spectrum features, whereas the lifetime is smaller than the typical value by approximately one order of magnitude.

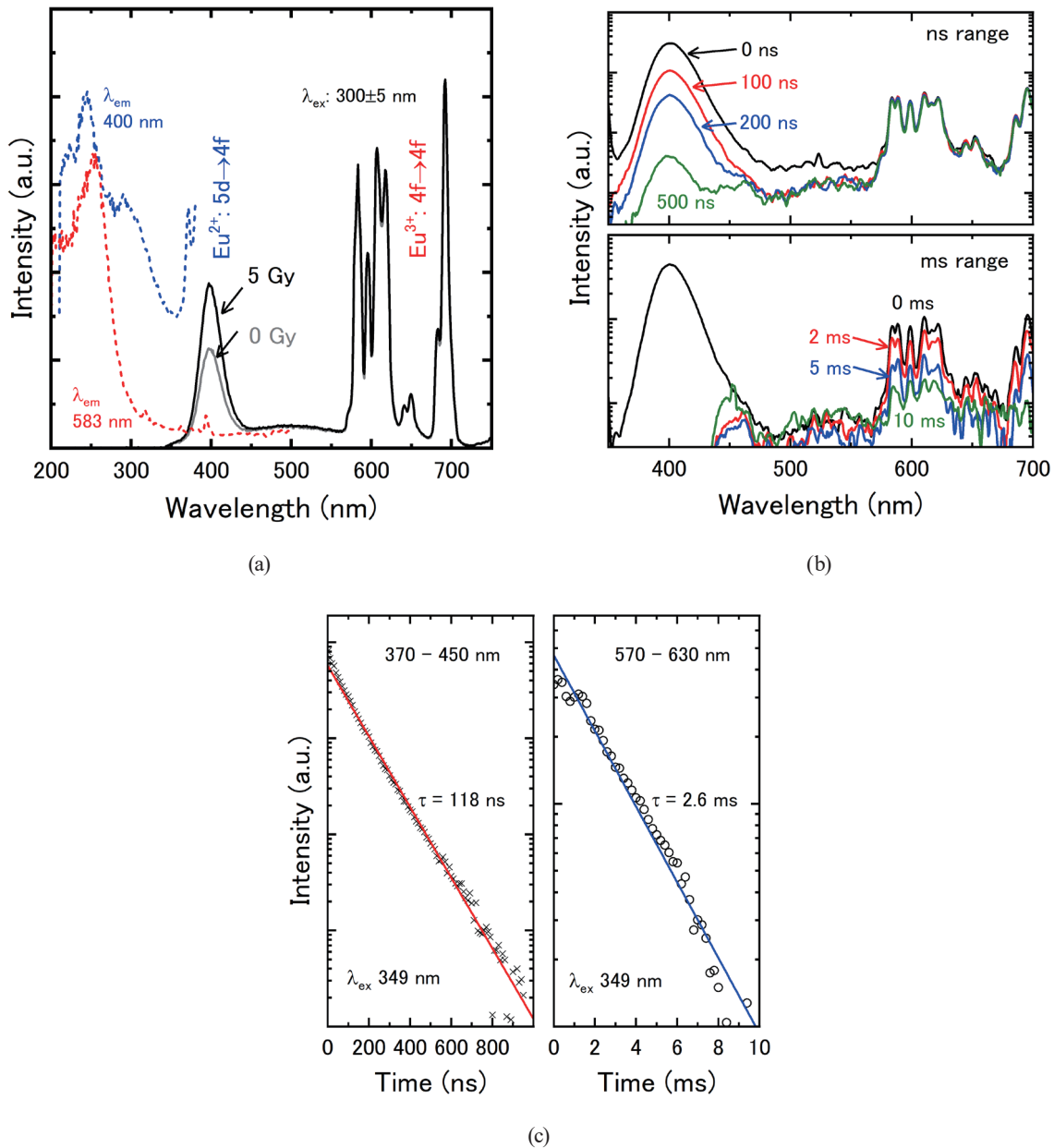


Fig. 1. (Color online) PL properties of Eu-doped CaBPO₅. (a) PL excitation and emission spectra measured before and after X-ray irradiation (5 Gy), (b) time-resolved PL spectra, and (c) PL decay curves.

The lifetime appeared to be smaller because the probability of nonradiative transition is high in this system. Note that earlier studies on Eu-doped CaBPO₅ reported the same emission at 400 nm, whose origin is assigned to Eu²⁺.⁽³⁰⁾

It is considered that the emission intensity of Eu²⁺ increases, whereas that of Eu³⁺ decreases after X-ray irradiation [see also Fig. 2(a)]. This indicates that the number of Eu²⁺ ions increases, whereas that of Eu³⁺ ions decreases following X-ray irradiation. Since Eu²⁺ as a luminescence center is formed by X-rays, it is considered that the Eu-doped CaBPO₅ exhibits RPL.

The RPL of Eu-doped CaBPO_5 has been considered for dosimetric applications, and representative properties are illustrated in Fig. 2. In particular, Fig. 2(a) demonstrates a dose response curve. Here, the doping concentration of Eu is 0.1%. It shows that the response (which is the integrated PL intensity between 350 and 450 nm induced by X-ray irradiation) monotonically increases with the radiation dose. The intersection of the dose response curve with the 3σ line is about 4 Gy, which is the lowest detection limit (LDL) with the present environment. Note that LDL varies with the type of reader system used. The present reader used is TORAIMS, in which the LDL of a commercially available Ag-doped phosphate glass is about

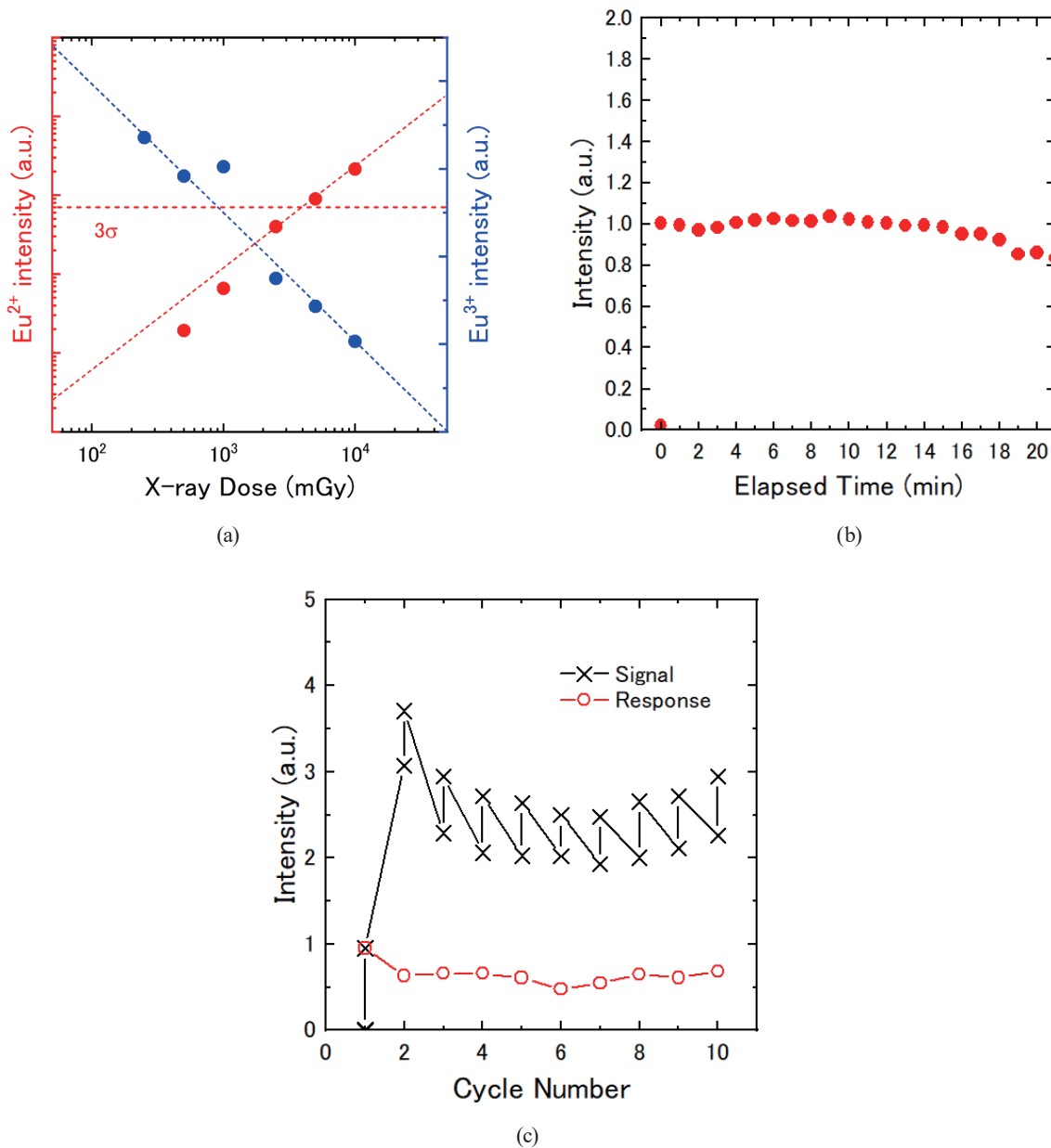


Fig. 2. (Color online) Dosimetric properties of RPL of 0.1% Eu-doped CaBPO_5 . (a) Dose response curve, (b) stability after X-ray irradiation, and (c) reproducibility.

5 mGy, whereas the LDL obtained by using the optimized commercially available reader is about 10 μ Gy.

Figure 2(b) shows the stability of RPL, which is equivalent to the Eu^{2+} center formed by the X-ray irradiation of 10 Gy. It is seen that the response value decreases by about 20% of its original value after 20 min, whereas the majority of the signal remains after the dose. Therefore, it can be considered that the RPL signal is reasonably stable, and no sign of buildup is observed. Thus, the RPL of Eu-doped CaBPO_5 can be considered for real-time dose monitoring.^(31,32)

Figure 2(c) demonstrates the reproducibility of RPL. For the characterization, the X-ray irradiation of 5 Gy was performed first to record the response value, then the sample was heat-treated at 500 °C for 100 s to reverse the response signal. These treatments were repeated 10 times to study the reproducibility of RPL. As illustrated in Fig. 2(c), in the first cycle, the signal intensity increases after irradiation. After heat treatment, it considerably increases, so the initial value of the second cycle is about three times larger than that of the first cycle after irradiation. After the irradiation of the second cycle, the intensity increases further; then, the following heat treatment effectively decreases the signal, unlike the first behavior. Despite the fluctuation of the signal by heat treatment, the response value, which is an increased signal after X-ray irradiation, is almost consistent regardless of the treatment cycle. Therefore, the RPL itself is reasonably reproducible.

4. Conclusions

Eu-doped CaBPO_5 was synthesized by the solid-state reaction route, and then it was confirmed that it exhibits RPL due to the valence change of the Eu ion ($\text{Eu}^{3+} \rightarrow \text{Eu}^{2+}$) induced by radiation. In addition, the dosimetric properties of RPL were studied: the PL intensity of Eu^{2+} increases as a function of dose and is stable over 20 min, RPL can be reversed by heat treatment (500 °C for 100 s), and RPL is reproducible multiple times.

Acknowledgments

This work was supported by a Grant-in-Aid for Scientific Research (B) (22H02009) from the Ministry of Education, Culture, Sports, Science and Technology of the Japanese government (MEXT) and the Research Center for Biomedical Engineering.

References

- 1 G. Okada: J. Ceram. Soc. Jpn. **129** (2021) 419. <https://doi.org/10.2109/jcersj2.21056>
- 2 G. Okada, Y. Koguchi, T. Yanagida, S. Kasap, and H. Nanto: Jpn. J. Appl. Phys. **62** (2023) 010609. <https://doi.org/10.35848/1347-4065/ac9023>
- 3 T. Yanagida, G. Okada, and N. Kawaguchi: J. Lumin. **207** (2019) 14. <https://doi.org/10.1016/j.jlumin.2018.11.004>
- 4 R. Yokota, S. Nakajima, and E. Sakai: Health Phys. **5** (1961) 219. <https://doi.org/10.1097/00004032-196105000-00014>
- 5 T. Kurobori, Y. Miyamoto, Y. Maruyama, T. Yamamoto, and T. Sasaki: Nucl. Instrum. Methods Phys. Res., Sect. B **326** (2014) 76. <https://doi.org/10.1016/j.nimb.2013.08.011>
- 6 S. W. S. McKeever, S. Sholom, and N. Shrestha: Radiat. Meas. **123** (2019) 13. <https://doi.org/10.1016/j.radmeas.2019.02.009>

- 7 M. Levita, T. Schlesinger, and S. S. Friedland: IEEE Trans. Nucl. Sci. **23** (1976) 667. <https://doi.org/10.1109/tns.1976.4328325>
- 8 A. Mrozik, P. Bilski, B. Marczevska, B. Obryk, K. Hodyr, and W. Gieszczyk: Radiat. Meas. **71** (2014) 31. <https://doi.org/10.1016/j.radmeas.2014.05.013>
- 9 G. M. Akselrod, M. S. Akselrod, E. R. Benton, and N. Yasuda: Nucl. Instrum. Methods Phys. Res., Sect. B **247** (2006) 295. <https://doi.org/10.1016/j.nimb.2006.01.056>
- 10 M. Akselrod and J. Kouwenberg: Radiat. Meas. **117** (2018) 35. <https://doi.org/10.1016/j.radmeas.2018.07.005>
- 11 G. Belev, G. Okada, D. Tonchev, C. Koughia, C. Varoy, A. Edgar, T. Wysokinski, D. Chapman, and S. Kasap: Phys. Status Solidi C. **8** (2011) 2822. <https://doi.org/10.1002/pssc.201084103>
- 12 S. Vahedi, G. Okada, B. Morrell, E. Muzar, C. Koughia, A. Edgar, C. Varoy, G. Belev, T. Wysokinski, D. Chapman, and S. Kasap: J. Appl. Phys. **112** (2012) 073108. <https://doi.org/10.1063/1.4754564>
- 13 A. Edgar, C. R. Varoy, C. Koughia, G. Okada, G. Belev, and S. Kasap: J. Non-Cryst. Solids **377** (2013) 124. <https://doi.org/10.1016/j.jnoncrysol.2012.12.022>
- 14 V. Martin, G. Okada, D. Tonchev, G. Belev, T. Wysokinski, D. Chapman, and S. Kasap: J. Non-Cryst. Solids **377** (2013) 137. <https://doi.org/10.1016/j.jnoncrysol.2012.12.015>
- 15 S. Vahedi, G. Okada, C. Koughia, R. Sammynaiken, A. Edgar, and S. Kasap: Opt. Mater. Express **4** (2014) 1244. <https://doi.org/10.1364/ome.4.001244>
- 16 G. Okada, Y. Fujimoto, H. Tanaka, S. Kasap, and T. Yanagida: J. Rare Earths **34** (2016) 769. [https://doi.org/10.1016/s1002-0721\(16\)60092-3](https://doi.org/10.1016/s1002-0721(16)60092-3)
- 17 G. Okada, N. Kawaguchi, S. Kasap, H. Nanto, and T. Yanagida: Radiat. Meas. **132** (2020) 106251. <https://doi.org/10.1016/j.radmeas.2020.106251>
- 18 G. Okada, N. Ikenaga, Y. Koguchi, T. Yanagida, S. Kasap, and H. Nanto: Mater. Res. Bull. **159** (2023) 112107. <https://doi.org/10.1016/j.materresbull.2022.112107>
- 19 S. Asada, G. Okada, T. Kato, F. Nakamura, N. Kawano, N. Kawaguchi, and T. Yanagida: Chem. Lett. **47** (2018) 59. <https://doi.org/10.1246/cl.170940>
- 20 G. Okada, K. Shinozaki, D. Shiratori, N. Kawaguchi, and T. Yanagida: Ceramics Int. **45** (2019) 9376. <https://doi.org/10.1016/j.ceramint.2018.08.027>
- 21 Y. Kohara, G. Okada, I. Tsuyumoto, E. Kusano, and H. Nanto: Mater. Lett. **303** (2021) 130502. <https://doi.org/10.1016/j.matlet.2021.130502>
- 22 Y. Kohara, G. Okada, I. Tsuyumoto, and H. Nanto: J. Mater. Sci.: Mater. Electron. **34** (2023) 472. <https://doi.org/10.1007/s10854-022-09759-5>
- 23 Y. Fujimoto, G. Okada, D. Sekine, T. Yanagida, M. Koshimizu, H. Kawamoto, and K. Asai: Radiat. Meas. **133** (2020) 106274. <https://doi.org/10.1016/j.radmeas.2020.106274>
- 24 G. Okada, T. Kojima, J. Ushizawa, N. Kawaguchi, and T. Yanagida: Curr. Appl. Phys. **17** (2017) 422. <https://doi.org/10.1016/j.cap.2017.01.004>
- 25 F. Nakamura, T. Kato, D. Nakauchi, G. Okada, N. Kawano, N. Kawaguchi, and T. Yanagida: Chem. Lett. **46** (2017) 1383. <https://doi.org/10.1246/cl.170580>
- 26 G. Okada, Y. Koguchi, T. Yanagida, and H. Nanto: Mater. Today Commun. **24** (2020) 101013. <https://doi.org/10.1016/j.mtcomm.2020.101013>
- 27 Y. Koguchi, G. Okada, S. Ueno, C. Sawai, and H. Nanto: J. Mater. Sci.: Mater. Electron. **34** (2023) 1972. <https://doi.org/10.1007/s10854-023-11410-w>
- 28 T. Kurobori, Y. Yanagida, and Y. Q. Chen: Jpn. J. Appl. Phys. **55** (2016) 02BC01. <https://doi.org/10.7567/jjap.55.02bc01>
- 29 G. Okada, K. Hirasawa, T. Yanagida, and H. Nanto: Sens. Mater. **33** (2021) 2117. <https://doi.org/10.18494/sam.2021.3327>
- 30 H. Liang, Q. Zeng, Y. Tao, S. Wang, and Q. Su: Mater. Sci. Eng., B **98** (2003) 213. [https://doi.org/10.1016/s0921-5107\(03\)00034-5](https://doi.org/10.1016/s0921-5107(03)00034-5)
- 31 T. Kurobori: Jpn. J. Appl. Phys. **57** (2018) 106402. <https://doi.org/10.7567/jjap.57.106402>
- 32 S. W. S. McKeever, S. Sholom, N. Shrestha, and D. M. Klein: Radiat. Meas. **132** (2020) 106246. <https://doi.org/10.1016/j.radmeas.2020.106246>